Scientific Papers. Series E. Land Reclamation, Earth Observation & Surveying, Environmental Engineering. Vol. XIII, 2024
Print ISSN 2285-6064, CD-ROM ISSN 2285-6072, Online ISSN 2393-5138, ISSN-L 2285-6064

ANALYSIS OF LANDSAT AND SENTINEL SATELLITE IMAGES FOR ROȘIA POIENI QUARRY AND VALEA ȘESII DECANTATION POND

Sorin HERBAN[1], Clara-Beatrice VÎLCEANU[1], Andrei CRIȘAN[2], Livia NISTOR-LOPATENCO[3]

[1]Politehnica University Timisoara, Civil Engineer Faculty, Department of Overland Communication Ways, Foundations and Cadastral Survey, 1 Ioan Curea Street, Timisoara, Romania
[2]Politehnica University Timisoara, Civil Engineer Faculty, Department of Steel Structures and Structural Mechanics, 2 Traian Lalescu Street, Timisoara, Romania
[3]Technical University of Moldova, Faculty of Construction, Geodesy and Cadastre, 41 Dacia Blvd, Chisinau, Republic of Moldova

Corresponding author email: beatrice.vilceanu@upt.ro

Abstract

Taking into consideration the valuable spectral information and its wide coverage, satellite remote sensing is an efficient and accurate instrument to analyse and monitor the Earth`s surface over time, even the negative consequences of anthropic activities. The present paper aims at monitoring in time the Roșia Poieni quarry and the negative effects resulting from the copper and gold exploitation, which led to the existence of the Valea Șesii tailing pond. To this purpose, Landsat satellite images were analysed over a 30-year period from platforms that offer free downloads. Image processing consisted of cropping the images according to the area of interest, applying the RGB combination and classifying them in order to obtain the surfaces. Moreover, indices for vegetation and water were applied for the images taken in 2018, 2020 and 2022. In order to obtain a more realistic image and to observe the differences, for the specified years, namely 2018, 2020 and 2022, Sentinel satellite images were processed in parallel. Despite the small size of the study area, satellite remote sensing has succeeded in delivering plausible, noteworthy results with great emphasis on hard-to-reach areas.

Key words*: image processing, mining, monitoring, remote sensing, tailing pond.*

INTRODUCTION

The Roșia Poieni quarry (Figures 1 and 2) is a surface copper mine in the Apuseni Mountains, located in Lupșa commune, Alba County, Transylvania area, Romania. The main storage location for tailings from mining is the Valea Șesii pond (Figure 2). The area's topography is characterized by rocky relief, deep valleys, and hanging platforms caused by the presence of facies formations that highlight specific volcanic regimes. On the slopes of the valley, there are several irregularities, including some negative shapes and sloughs, both on the platforms and in the meadows or on the terraces of the valley. The lands are regularly damaged by erosions, due to the high value of relief energy, displayed mainly altitudes starting from 400 m to 900 m, and the poor consistency of the clays and Senonian marls that mostly cover the surrounding region of deposit.

Figure 1. Location of the study area (https://geoportal.ancpi.ro/geoportal/imobile/Harta.html, https://harti.wansait.com/ro_ro/2012/judetul-alba-harta-administrativa-interactiva/)

The pond does not have a drainage system, so the quality indicators of the discharged water are frequently exceeded. Thus, the entire area is affected by both the quality of the water and the solvents found in the tributaries that flow into the Aries River and affect. In addition to this phenomenon, there are also negative effects in the area at the exit of the tailings, through

which sulfuric acid and heavy metal sulphates end up in water and soil, generating intense pollution of the Aries River Basin (Moldovan et al., 2021; Popa et al., 2015).

Figure 2. Roșia Poieni quarry (top photo https://mapio.net/pic/p-26288806/) and Valea Șesii tailing pond (bottom photo https://adevarul.ro/stiri-locale/alba-iulia/foto-satul-idilic-din-apuseni-disparut-sub-o-1883658.html)

The exploitation of the quarry began in 1978, the copper production in 1983 and the storage of the residues resulting from the exploitation was carried out in the village of Geamăna, due to its proximity and relief. In almost 40 years of waste storage, the village of Geamăna was transformed into a colourful and toxic desert of chemical sludge and heavy metals, of which only the steeple of the sunken village church remains (Toderaș, 2021) (Figure 3).

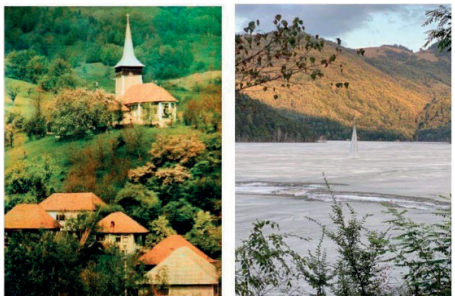

Figure 3. The steeple of the sunken church in Geamăna village (before and after) https://www.dailymail.co.uk/travel/travel_news/article-4596446/Amos-Chapple-captures-Romanian-s-Geamana-village.html

MATERIALS AND METHODS

Remote sensing from satellites of parameters waters has been extensively applied to lakes', rivers, seas' studies. Water remote sensing is based on the examination of the spectrum of optical active components of the upper layer of the water body, such as mineral content, turbidity, total suspended particles, and chlorophyll-a. Earth observation satellite data (e.g. Landsat, Sentinel) available for free can provide valuable information for evaluating huge areas, however, the quality and frequency of data transmission can vary (Makri, 2016).

In order to download the necessary satellite images (Mendez Garzón & Valánszki, 2020), the Earth Explorer platform - USGS (United States Geological Survey) was used (https://www.usgs.gov/landsat-missions).

Firstly, the study area was specified, then the criteria of interest, namely the period, the type of satellite, and the degree of cloud coverage. For the processing, the following images from the summer-autumn period have been downloaded:

- year 1992, Landsat 4-5 satellites data;
- year 2000, Landsat 7 satellite data;
- year 2014, Landsat 8 satellite data;
- year 2018, Landsat 8 satellite data;
- year 2020, Landsat 8 satellite data;
- year 2022, Landsat 9 satellite data.

To download the satellite images from the Copernicus platform, the study area was first chosen by drawing a polygon to include it, then the following criteria were selected: the period, the type of satellites and the degree of cloud coverage. Images that were not available at the time were added to the cart and downloaded shortly after they were available.

The following images were taken and processed:

- the years 2016, 2018, 2020 and 2022, data taken with Sentinel 1 to apply corrections and orthorectifications.
- the years 2018, 2020 and 2020, data retrieved with Sentinel 2 for their classification and application of water and vegetation indices (https://sentinels.copernicus.eu/web/sentinel/home).

Landsat and Sentinel data have been used in this case study as satellite sensors operate on various spatial, spectral, and temporal

resolutions. In particular, the Copernicus Emergency Management Service (CEMS) makes substantial use of Sentinel-1 data, as SAR equipment' ability to identify flooded areas, see through clouds or dense smoke, and detect land changes is especially important in emergency situations. Sentinel-1 SAR data eases the identification of alterations in topography and infrastructure damage after urban disasters, allowing for more precise assessments that are critical for recovery planning and community impact evaluation.

Landsat images processing

The Landsat satellite images have been further processed. In order to achieve the RGB combination, it was necessary to know the correspondence between the bands of the Landsat satellites and the area of the electromagnetic spectrum. Thus, bands 3, 2 and 1 were used for images taken with Landsat 4, 5 and 7 satellites, and bands 4, 3 and 2 were used for images taken with Landsat 8 and 9 satellites.

The steps before performing the RGB combination (Badulescu et al., 2019) consisted of importing the downloaded images in tiff format and cropping them according to the area of interest. Applying the RGB combination to all the data that correspond to each year of the change monitor (Hila et al., 2018) produces the Figure 4.

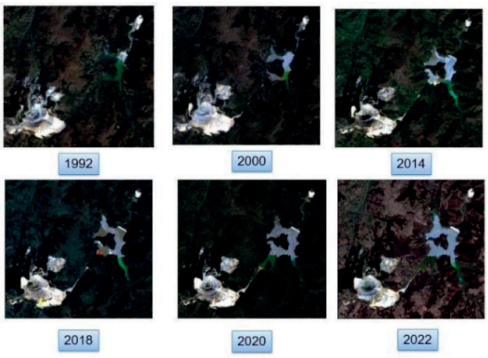

Figure 4. RGB combination for Landsat images

To achieve the supervised classification, the following steps are followed:

- Sampling - the stage in which the operator intervenes to identify and define each sample;
- Classification - involves placing each pixel in the right class. This step is the most important because the computer uses predefined decision rules to identify each pixel in the image (Basayigit & Ersan, 2015);
- Obtaining the final product or presenting the result in the form of thematic maps or tables corresponding to the recording of the scene (Iosub, 2012).

Choosing samples was realized based on the classification scheme (Table 1), by choosing the class categories that contain the number, type of information classes and their description.

Table 1. Images classification scheme

No.	Sample	Sample description
1	forest	Area with dense tree layer
2	pasture land	Area covered with grassy vegetation
3	quarry	Exploitation area
4	water	The amount of water resulting from settling
5	tailings	The amount of acidic water with high content of toxic substances
6	sludge	The amount of toxic mineral sediments

The creation of the samples was carried out using the cropped true colour RGB 321 and RGB 432 composite images for each year. From the "Supervised" menu, the "Signature Editor" window was opened, and the samples were vectorized using the "polygon" function (Figure 5).

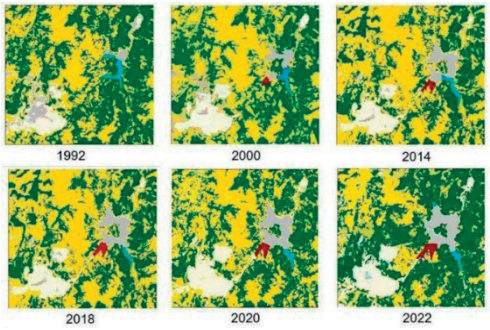

Figure 5. Supervised classification for Landsat images

Unsupervised classification is based on spectral classes (pixel values) or clusters in a multiband image or individual pixel values. The more classes there are, the number of iterations for the algorithm increases.

In the Erda's Imagine 2015 program, the unsupervised classification was realized from

the "Raster" menu, the sequence "Classification - Unsupervised - Unsupervised Classification". The total area of the study that was covered by Landsat satellite images is 4158 ha. To determine surface changes over the years (Vorovencii, 2015), the number of pixels corresponding to each class was multiplied by 0.09 ha. The surfaces that resulted are presented in Table 2.

Table 2. Surfaces obtained from processing Landsat satellite images

	1992	2000	2014	2018	2020	2022
	(Hectares)					
Forest surface	1930.48	1970.04	2060.59	2026.48	2025.46	2102.95
Pastureland surface	1854.77	1747.01	1716.90	1658.03	1657.19	1586.44
Quarry surface	302.38	342.95	323.22	310.56	301.47	284.58
Water surface	57.41	22.54	28.19	17.80	18.06	16.36
Tailings surface	0	10.06	16.76	20.81	26.09	24.29
Sludge surface	12.95	65.38	102.51	124.30	129.71	143.36

Sentinel images processing

Pre-processing Sentinel1 images using SNAP software involved, firstly, identifying the study area in the image and cutting it according to a drawn rectangle that includes the entire studied area. The image pre-processing process (Herbei et al., 2023) involved the following steps: radiometric calibration - betaO type calibration; Earth curvature correction and noise removal (Figure 6), for the image that was previously calibrated, resulting the final image (Figure 7) after the orthorectification.

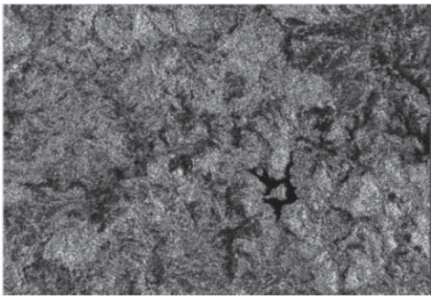

Figure 6. The 2022 Sentinel image after noise removal

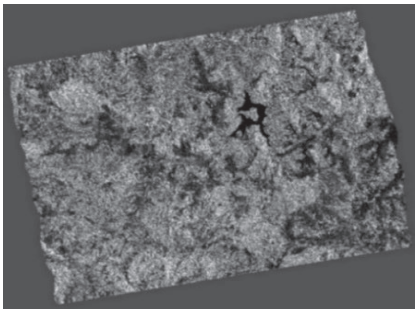

Figure 7. The 2022 Sentinel image after applying all corrections

To achieve the RGB combination of satellite images taken with Sentinel 1, the Gamma_VH band is used for the red band, the Gamma_VV band for the green band and Gamma_VH/Gamma_VV band was used for the blue band. For a better processing of the images and obtaining better quality results, images taken with the Sentinel 2 satellite were also downloaded, the continuation of the study being based on the results obtained after their processing. In this case, the combination of bands that correspond to RGB consists of bands 4, 3, and 2, respectively (Figure 8).

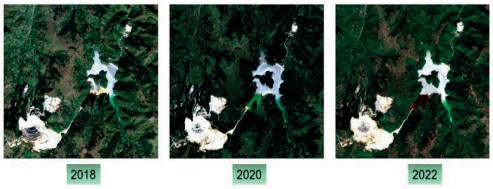

Figure 8. RGB combination for the years 2018, 2020, 2022

For the supervised classification of Sentinel satellite images, the Maximum Likelihood algorithm was used, which assumes that pixels are assigned to the class with the highest probability. To create the samples, the classes described in the classification scheme in Table 1 were used. The sampled areas represent groups of pixels that include the characteristic elements necessary to identify and separate the classes (Figure 9). Vector layers were created for each class and areas defining the class were vectorized and then assigned to them. Figure 10 shows the result of the supervised classification.

Unsupervised Media - K classification was used for this study. This algorithm combines

"observations" (pixels) and places them into discrete groups. Pixel placement is realized by creating nodes that are placed in the center of the cluster.

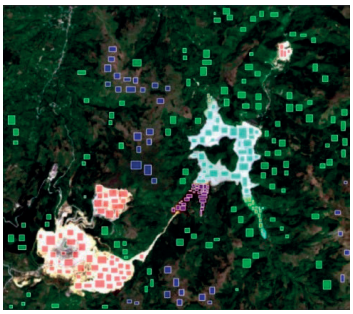

Figure 9. Sampling creation

The node is positioned so that the distance between the node and the closest point is less than the distance between these points and the next node. A number of 14 classes were chosen that were automatically customized based on algorithms. The difference between this method and supervised classification is that in the latter spectral signatures chosen by the user are used (Figure 11).

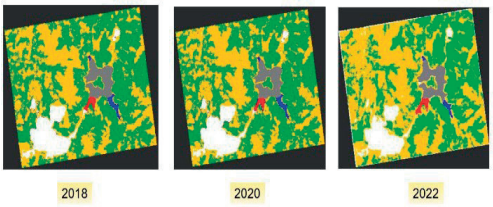

Figure 10. Supervised classification for images corresponding to the years 2018, 2020 and 2022

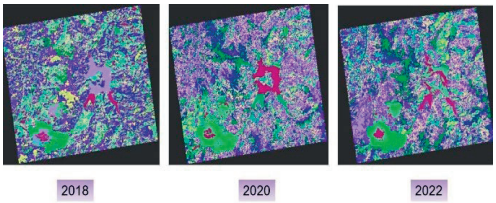

Figure 11. Unsupervised classification for images corresponding to the years 2018, 2020 and 2022

For the Sentinel images, the surfaces were also determined, from which the percentages representing the degree of coverage of each class were taken (Table 3).

Table 3. Surfaces obtained from processing Sentinel satellite images

	2018	2020	2022
	(Hectares)		
Forest surface	2322.39	2325.74	2427.83
Pasture land surface	1917.90	1912.38	1815.61
Quarry surface	309.22	300.12	283.98
Water surface	17.98	18.35	17.02
Tailings surface	20.96	26.35	24.68
Sludge surface	124.68	130.21	144.02

RESULTS AND DISCUSSIONS

Once the surfaces have been obtained, the following were concluded:

- throughout the 30 years, the forest surface has increased, and the forest area has started to gain ground over the pastures;
- the tailings surface in the settling pond and the sludge surface have increased significantly, the result being worrying;
- the surface of the quarry at the ground level decreases since exploitation is concentrated on depth and nature recovers land.

The next step consisted of studying the settling pond's surfaces, as well as the elements that make it up: tailings, water, and sludge (Figure 12). The surface of the tailing pond has increased considerably (Table 4), which has caused the compromise of people's habitat in the area.

Table 4. The evolution of the settling pond surfaces

	1992	2000	2014	2018	2020	2022
	(Hectares)					
Water surface	57.41	22.54	28.19	17.80	18.06	16.36
Tailing surface	0	10.06	16.76	20.81	26.09	24.29
Sludge surface	12.95	65.38	102.51	124.3	129.71	143.36
Tailing pond's surface	70.36	97.98	147.46	162.91	173.86	184.01

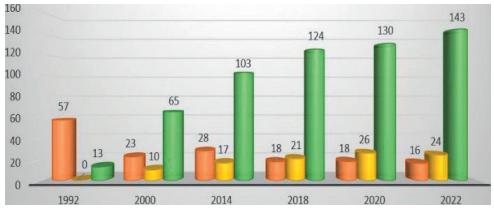

Figure 12. Time evolution of the Valea Şesii decantation pond (Red - Water surface, Orange - Tailing pond surface, Green - Sludge surface)

Normalized Difference Vegetation Index

The differential reflection between the red band and the near-infrared band allows density and intensity of green vegetation monitoring using the spectral reflectivity of solar radiation.

(Rouse et al.) Green leaves show a better reflection in the near infrared wavelength than in the visible spectrum. Leaves that are water-deficient or diseased or dead turn yellow and their reflectivity decreases greatly for the infrared wavelength.

For near-infrared and red, the corresponding bands are 4 and 3 for images taken with Landsat 4-5 and 7, and for images taken with Landsat 8 and 9 satellites, bands 5 and 4. The NDVI index was applied to images taken in 2018, 2020 and 2022, and after applying the formula, the resulting images were automatically generated. For the images resulted after applying the NDVI index to be interpretable, it was necessary to reclassify them. This was realized from the GIS Analysis menu, the Database Query - Reclass sequence. The images presented in Figure 13 and classification categories were thus obtained. As regards the images taken with Sentinel satellites, the bands used for the NDVI index are band 8 and band 4 (Figure 14).

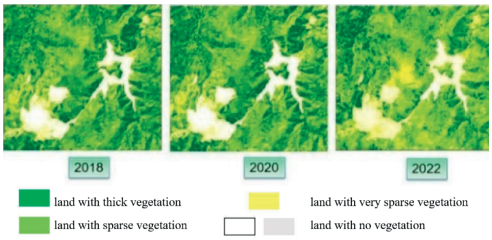

Figure 13. The Landsat images after applying the NDVI index and reclassified for the years 2018, 2020 and 2022

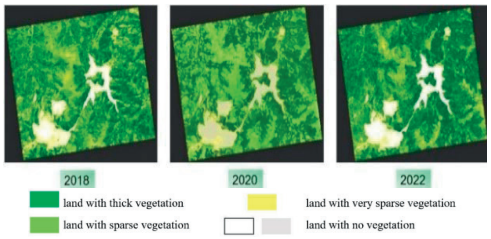

Figure 14. Sentinel images after applying the NDVI index and reclassified for the years 2018, 2020, 2022

Normalized Difference Water Index

The corresponding near-infrared and green bands are 4 and 5 for Landsat 4-5 and 7 images. Bands 5 and 6 were chosen for Landsat 8 and 9 images (Figures 15 and 16) (McFeeters, 1996).

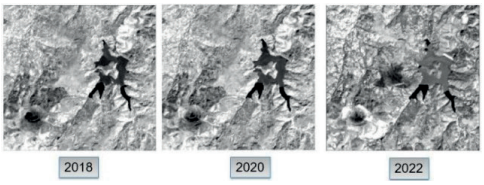

Figure 15. Landsat images resulting after applying the NDWI index for the years 2018, 2020 and 2022

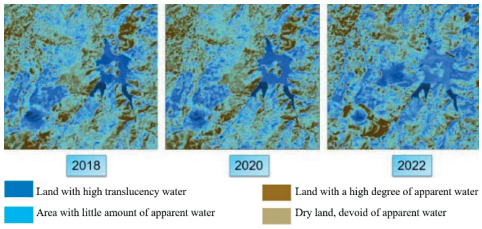

Figure 16. Landsat images after applying the NDWI index and reclassified for the years 2018, 2020 and 2022

For Sentinel satellite images, the appropriate bands for applying the NDWI index are band 8 and band 9 (Figure 17). The sequence used in the SNAP program is Raster - Band Maths. The specific formula, respectively (B8-B9)/(B8+B9) is written in the dialog box.

The values of the NDWI index are between -1 and +1, are presented in Figure 18 and are as follows:

- dark tons (values <0) express the sheen of the water;
- light tons (values >0) represent dry land.

A comparison of the processed images, both those taken with Landsat satellites and those taken with Sentinel satellites, was followed and presented in Figures 19, 20, 21 and 22.

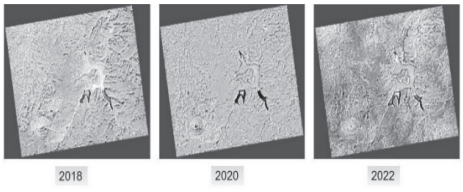

Figure 17. Sentinel images resulted after applying the NDWI index for the years 2018, 2020 and 2022

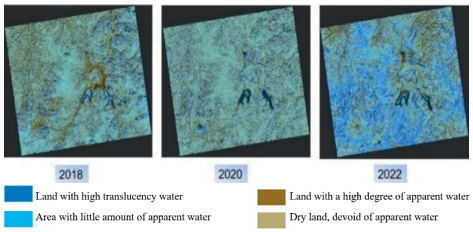

Figure 18. Sentinel images after applying the NDWI index and reclassified for the years 2018, 2020 and 2022

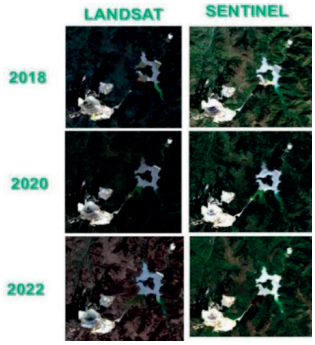

Figure 19. RGB combination for Landsat and Sentinel images

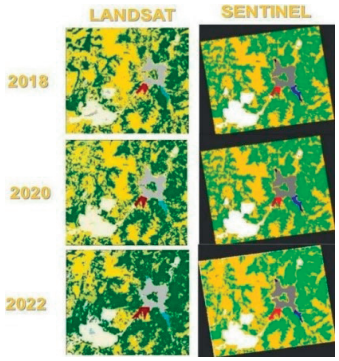

Figure 20. Classification of Landsat and Sentinel images

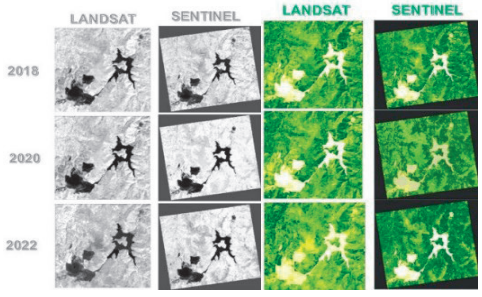

Figure 21. NDVI index and reclassified for the years 2018, 2020, 2022

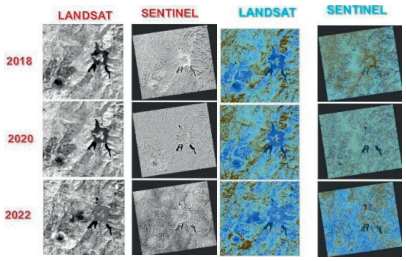

Figure 22. NDWI index and reclassified for the years 2018, 2020, 2022

The comparison of the Figure 23 with Figure 24 from the point of view of the surfaces concerned strictly the surface rendered by the settling pond.

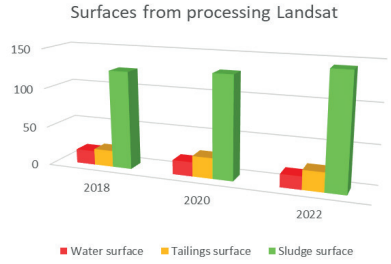

Figure 23. Tailings pond surfaces comparison for Landsat images

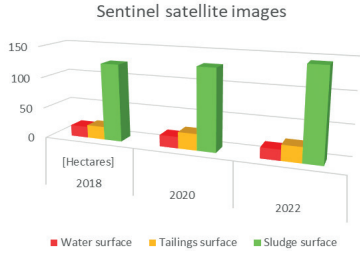

Figure 24. Tailings pond surfaces comparison for Sentinel images

CONCLUSIONS

The present article is a brief description of the workflow followed for the analysis of Landsat and Sentinel satellite images for Roșia Poieni quarry and Valea Șesii decantation pond.
Regarding the performance of combining multispectral and SAR (Sentinel and Landsat) satellite data for estimating both volumes and areas in the study area, Valea Sesii decantation pond, following the research carried out, it was found that:

✓ The quarry's surface at the ground level for the studied area has decreased in recent years because mining is focused on depth and nature is reclaiming land.
✓ The surface of the Valea Șesii settling pond has increased significantly, from 70.36 ha in 1992, to 184.01 ha in 2022.
✓ The number of tailings has increased considerably, currently occupying an area of 24.29 ha. This fact exerts a huge influence on the area, both now and in the future.
✓ Compared to Landsat images, those taken with Sentinel satellites have a slightly better spatial resolution, facilitating their processing.
✓ To obtain a higher quality of the processing results of the Sentinel 1 images, they must be pre-processed by applying various corrections.

From the analysed data it can be clearly seen that by using Sentinel SAR images it was possible to determine and continuously monitor the forest, pasture, water, tailing pond, quarry and sludge surface. The accuracy of the SAR water surface estimation was comparable to the NDWI given by Landsat. This data was validated by physical observations in the field, confirming that the protocols followed can be reliably applied and can be repeated.

Despite the small area of the study area, satellite remote sensing succeeds brilliantly in providing plausible results, worthy of consideration and of great importance over hard-to-reach areas.

REFERENCES

Badulescu, B., Matache, A.M., Vrancuta, L., Musat, S., Mircea, S., Petrescu, N. (2019). Shadows correction methods for Landsat satellite images. *Scientific Papers. Series E. Land Reclamation, Earth Observation & Surveying, Environmental Engineering*, *VIII*, 162-168, Print ISSN 2285-6064.

Basayigit, L., Ersan, R. (2015). Comparison of pixel-based and object-based classification methods for separation of crop patterns. *Scientific Papers. Series E. Land Reclamation, Earth Observation & Surveying, Environmental Engineering*, *IV,* 148-153, Print ISSN 2285-6064.

Herbei, M.V., Popescu, C.A., Bertici, R., Sala, F. (2023). Estimation of sunflower crop production based on remote sensing techniques. *Agrolife Scientific Journal*, *12*(1), 87-96.

Hila, A.S., Ferencz, Z., Cimpeanu, S. M. (2018). Land surface temperature monitoring through GIS technology using satellite Landsat images. *Scientific Papers. Series E. Land Reclamation, Earth Observation & Surveying, Environmental Engineering*, *VII,* 163-167, Print ISSN 2285-6064.

Iosub, F. (2012). Extracting spatial information from satellite images using supervised and unsupervised classifications, Geospatial seminars, geo-spatial.org.

Makri, S. (2016). Sentinel-2 and Landsat-7 satellite images qualitative comparison for evaluating advances in detecting lakes' quality parameters, Complementary certificate in Geomatics, Universite de Geneve, Institut de Sciences de L'Environnment.

McFeeters, S.K. (1996). The use of the Normalized Difference Water Index (NDWI) in the delineation of open water features. *Intern J of Remote Sensing, 17*(7), 1425–1432, https://doi.org/10.1080/01431169608948714.

Mendez Garzón, F.A., Valánszki, I. (2020). Remote sensing tendencies in the assessment of areas damaged by armed conflicts. *Scientific Papers. Series E. Land Reclamation, Earth Observation & Surveying, Environmental Engineering*, *IX,* 223-234, Print ISSN 2285-6064.

Moldovan, A., Török, A.I., Cadar, O., Roman, M., Roman, C., Micle, V. (2021). Assessment of toxic elements contamination in surface water and sediments in a mining affected area. *Studia Universitatis Babes-Bolyai Chemia*, *66*(2), 181-196, DOI10.24193/subbchem.2021.2.16.

Popa, M., Bostan, R., Ilie, N., Varvara, S. (2015). Natural sorbents used for the removal of heavy metals from acidic wastewaters generated at `Valea Sesei' tailing pond from Rosia Poeni mining perimeter (Romania). *J Environ Prot & Ecology*, *16*(3), 839-849.

Rouse, J. W., R. H. Haas, J. A. Schell, and D. W. Deering (1973). Monitoring vegetation systems in the Great Plains with ERTS, Third ERTS Symposium, NASA SP-351 I, 309-317.

Toderaș, M. (2021). Mining risks at exploitation in Roșia Poieni open pit mine, Romania. *Mining Revue*, 27(1), 1-11, ISSN-L 1220-2053 / ISSN 2247-8590, DOI: 10.2478/minrv-2021-0001.

Vorovencii, I. (2015). Habilitation Thesis: Identification, assessing and monitoring of environmental changes using remote sensing methods, available online at https://www.unitbv.ro/documente/cercetare/doctorat-postdoctorat/abilitare/teze-de-abilitare/vorovencii-iosif/05-vorovencii_Iosif-Teza_de_abilitare_RO.pdf

https://www.earthdata.nasa.gov/

https://sentinels.copernicus.eu/web/sentinel/home

https://www.usgs.gov/landsat-missions

https://static.eos.com/wp-content/uploads/2020/11/how-NDVI-works-EN.jpg

https://ro.wikipedia.org/wiki/Valea_%C8%98esii_(Lup%C8%99a),_Alba

https://mapio.net/pic/p-26288806/

https://adevarul.ro/stiri-locale/alba-iulia/foto-satul-idilic-din-apuseni-disparut-sub-o-1883658.html

https://static.eos.com/wp-con tent/uploads/2020/11/how-NDVI-works-EN.jpg)

https://harti.wansait.com/ro_ro/2012/judetul-alba-harta-administrativa-interactiva/

https://geoportal.ancpi.ro/geoportal/imobile/Harta.html